ELSEVIER

Journal of Molecular Structure: THEOCHEM 813 (2007) 49–56

THEO CHEM

www.elsevier.com/locate/theochem

Electronic and structural properties of the (001) $SrZrO_3$ surface

J.R. Sambrano [a,*], V.M. Longo [b], E. Longo [b], C.A. Taft [c,*]

[a] *Grupo de Modelagem e Simulação Molecular, DM, Universidade Estadual Paulista, P.O. Box 473, 17033-360 Bauru, SP, Brazil*
[b] *LIEC, DQ, UFSCar, P.O. Box 676, 13565-905, São Carlos, SP, Brazil*
[c] *Centro Brasileiro de Pesquisas Físicas, Rua Dr. Xavier Sigaud, 150, Urca, 22290-180, Rio de Janeiro, Brazil*

Received 22 January 2007; accepted 19 February 2007
Available online 22 February 2007

Abstract

The structural and electronic properties of $SrZrO_3$ selected surfaces were investigated by means of density functional theory applied to periodic calculations at B3LYP level. The relaxation effects for two symmetric and asymmetric terminations are analyzed. The electronic and energy band properties are discussed on the basis of band structure as well density of states. There is a more significant rumpling in the SrO as compared to the ZrO_2 terminated surfaces. The calculated indirect gap is 4.856, 4.562, 4.637 eV for bulk, ZrO_2 and asymmetric terminations, respectively. The gap becomes direct; 4.536 eV; for SrO termination. The contour in the (110) diagonal plane indicates a partial covalent character between Zr and O atoms for the SrO terminated surface.

Keywords: $SrZrO_3$; Perovskite; CRYSTAL; Periodic calculations; Surfaces; B3LYP

1. Introduction

There is an increasing interest in material research with potential technological applications, such as hydrogen sensors, fuel sensors and non-volatile random access memory devices. Among these materials, $AZrO_3$ (A = Ba, Sr, Pb) perovskites crystals have attracted considerable attention due to their ferroelectric and piezoelectric properties, yielding attractive models for experimental and theoretical academic research.

In recent years, zirconate perovskites have been the focus of experimental studies. Notwithstanding, substantial theoretical research has not been devoted to these materials. In particular, strontium zirconate, $SrZrO_3$ (SZ), is interesting because of its high-temperature electronic properties whereas phase transitions of SZ have been studied by Kennedy and co-workers using powder neutron diffraction and the Rietveld method [1]. These authors confirm the pathway for orthorhombic (970 K) to cubic phase (1400 K) transition. These compounds have a rather high melting temperature of approximately 2920 K [2]. The cubic phase is thus in the range of temperature where most of the applications of interest take place [3].

Computational studies, based on first principle calculations, can be important for elucidating the electronic and structural properties of materials [4–7]. Mete's group reported first principles calculations of the electronic properties of SZ, in its high-temperature cubic phase [3]. Terki at al. made full-potential linearized augmented plane wave (FP-LAPW) calculations and discussed structural, electronic and optical properties of $BaTiO_3$ and $SrZrO_3$ [8]. Evarestov end co-workers reported the results of density functional theory (DFT) LCAO and plane wave (PW) calculations of four known $SrZrO_3$ phases [9,10]. There are many publications of surface properties [11–14] but we do not have knowledge of studies performed on SZ surfaces. On the other hand, recent experiments suggest that even slabs only a few monolayers thick can exhibit ferroelectric ordering [15,16].

In this paper, we report periodic first principle calculations based on density functional theory in order to investigate the structural and electronic properties of cubic

* Corresponding authors. Tel.: +551431036086; fax: +551431036096.
E-mail addresses: sambrano@fc.unesp.br (J.R. Sambrano), taft@superig.com.br (C.A. Taft).

0166-1280/$ - see front matter © 2007 Elsevier B.V. All rights reserved.
doi:10.1016/j.theochem.2007.02.022

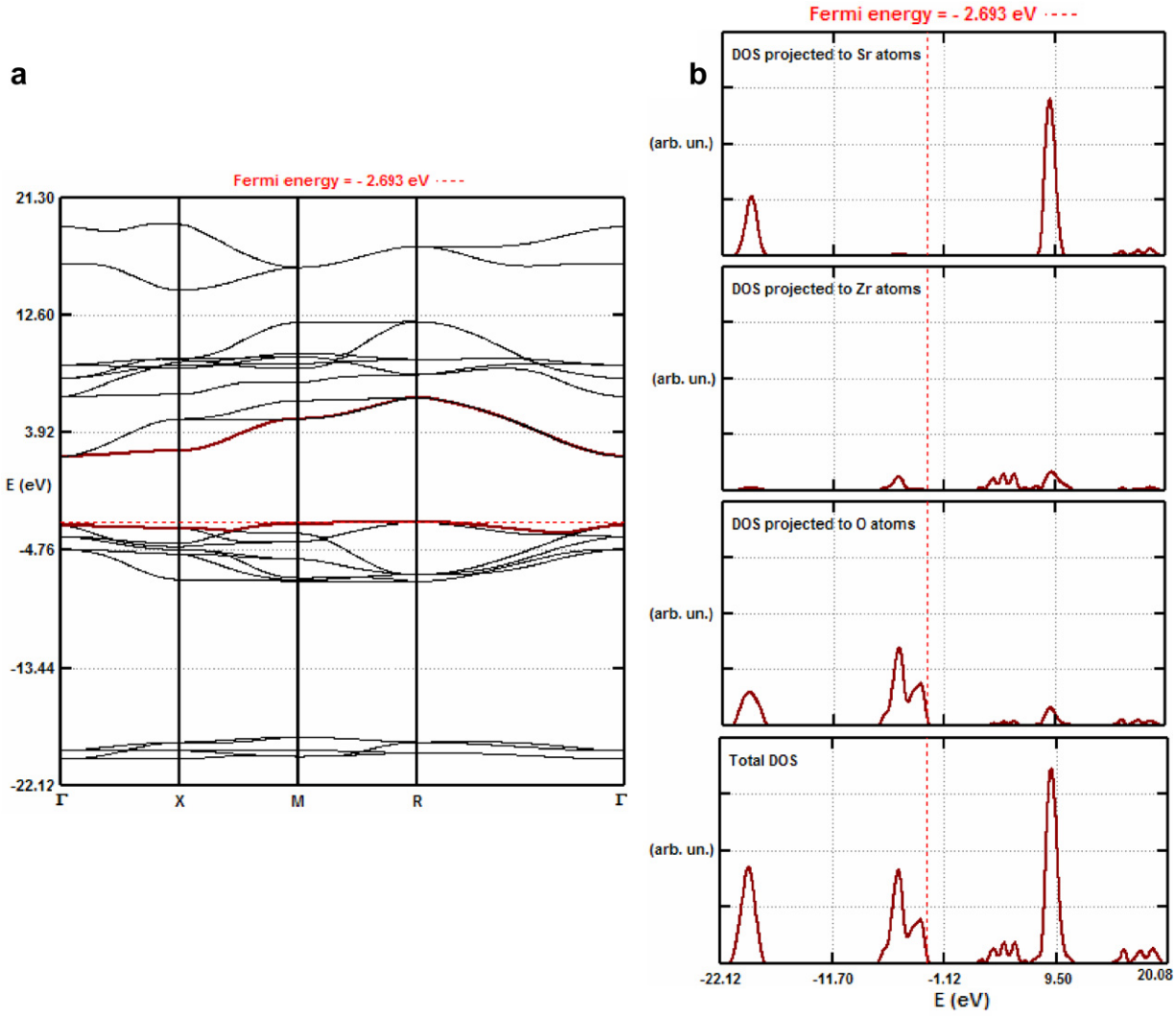

Fig. 1. Band structure (a) and DOS (b) of bulk $SrZrO_3$.

Table 1
Calculated optical gap (in eV) for the bulk and ZrO_2, SrO and asymmetric terminations

	Bulk	ZrO_2 termination	SrO termination	Asymmetric termination
Γ–Γ	5.070	4.955	*4.536*	4.663
M–M	5.660	7.229	7.776	4.971
X–X	7.705	5.206	5.583	7.248
R–R	9.175	–	–	–
R–Γ	*4.856*	–	–	–
R–X	7.622	–	–	–
M–Γ	5.262	*4.562*	4.614	*4.637*
X–Γ	4.93	4.916	4.612	4.588

$SrZrO_3$ in the bulk and (001) surface structures. The results are discussed in terms of density of states, band structures, charge distributions and compared with reported quantum mechanical calculations as well as available experimental data.

2. Computational method and model system

The periodic DFT calculations with the B3LYP hybrid functional [17,18] were made using the CRYSTAL03 computer code [19]. The B3LYP functional is known to simulate the energetic, geometric, and electronic properties of materials with significantly greater accuracy [20]. This functional has been successfully employed for studies of the electronic and structural properties of diverse compounds [4], including Ba(Pb)TiO_3 [7,12,21] systems.

Calculation schemes and basis sets for Sr, Zr and O centers can be found at the CRYSTAL home page [22].

In the $SrZrO_3$ cubic structure, the Sr atoms share the vertices of the unit cell and the Zr atoms are located at the center, surrounded by six O atoms occupying the face centers in an octahedral configuration. The experimental value for the lattice constant a is 4.109 Å [23] and the theoretical lattice constant which minimizes the energy of the structure when the ions are fixed in the cubic structure is $a = 4.144$ Å. Our theoretical lattice constant is only

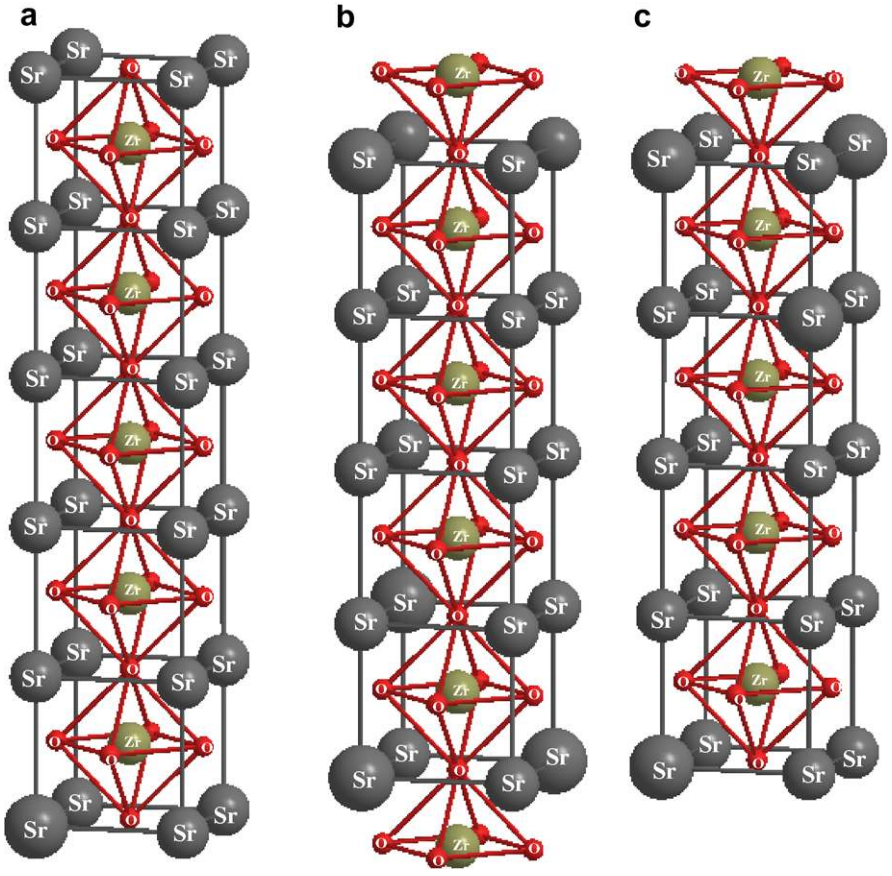

Fig. 2. (a) SrO, (b) ZrO_2 and (c) asymmetric terminated slab of $SrZrO_3$.

Table 2
Calculated cleavage energies, E_s^u (eV/cell), relaxation energies, $E_{rel}(i)$ (eV/cell), and surface energies, $E_s(i)$ (eV/cell) where i denotes SrO or ZrO_2

	5	7	9	11	13	15
E_s^u	1.99	1.90	1.97	1.97	1.96	1.96
$E_{rel}(ZrO_2)$	−0.19	−0.22	−0.22	−0.22	−0.22	−0.22
$E_{rel}(SrO)$	−0.75	−0.79	−0.80	−0.80	−0.79	−0.83
$E_s(ZrO_2)$	1.80	1.68	1.75	1.75	1.74	1.74
$E_s(SrO)$	1.24	1.11	1.17	1.17	1.17	1.17

0.0085% larger than experimental value and in good agreement with other theoretical results [1,8,10]. Nelder-Mead (SIMPLEX) [24] method have been used to perform the optimization of cell parameter.

The bulk modulus, B, was evaluated as the quadratic coefficient of polynomial fits to the total energy, i.e., $B = \frac{2}{9V_o}\frac{\partial E_{un.cell}}{\partial V_2}$ [19,25]. The calculated values of $B = 190$ GPa, is overestimated with respect to the experimental values of 150 GPa [26] and underestimated by 15% for a series of Zr perovskites [3,27].

There is no a unique method to evaluated the bulk modulus, several widely used analytic forms for the equation of state is presented by Alchagirov [28] and co-workers. The choice of a given method is useful in comparing the results performed using others ways.

The band structures were obtained for 80 $\vec{k}$ points along the appropriate high-symmetry paths of the adequate Brillouin zone. Diagrams of the density of states (DOS) have been made for analysis of the corresponding electronic structure. The XcrysDen program [29] has been used for the band structure diagram, DOS and charge density maps.

Table 3
Displacements of atoms, δz, of all layers from their perfect lattice positions (in Å) for ZrO_2, SrO and asymmetric terminations slabs

	ZrO_2 termination		SrO termination		Asymmetric termination		
1st layer	Zr −0.15	O −0.14	Sr −0.46	O −0.05	Zr −0.15 (Zr −0.02)^{7th}	–	O −0.15 (O 0.01)^{7th}
2nd layer	Sr 0.11	O −0.03	Zr 0.04	O −0.06	–	Sr 0.11 (Sr 0.14)^{8th}	O −0.04 (O 0.02)^{8th}
3rd layer	Zr −0.06	O −0.06	Sr −0.15	O −0.04	Zr −0.07 (Zr −0.05)^{9th}	–	O −0.07 (O 0.04)^{9th}
4th layer	Sr 0.02	O −0.02	Zr −0.01	O −0.03	–	Sr 0.03 (Sr 0.43)^{10th}	O −0.03 (O 0.03)^{10th}
5th layer	Zr −0.02	O −0.02	Sr −0.04	O −0.01	Zr −0.04	–	O −0.01
6th layer (Central)	Sr 0.00	O 0.00	Zr 0.00	O 0.00	–	Sr 0.05	O −0.01

Values in parenthesis are the displacement of the 7th, 8th, 9th and 10th layers of asymmetric model.

3. Results and discussions

3.1. Bulk properties

Fig. 1 represents the band structure and the projected DOS of the bulk $SrZrO_3$. The calculated optical band gaps are summarized in Table 1. The top of the valence band (VB) of the Brillouin zone, is coincident with the Fermi energy, 2.693 eV, is located at R point. The band gap is indirect, 4.856 eV, between R and Γ points. This value is smaller that the experimental observed gap, 5.08 eV [30] and ~5.6 eV [31]. The value of direct gap between Γ and Γ points is 5.07 eV. The conduction band (CB) bands between Γ and X points are flat. An analysis of the principal AO component of selected bands indicates that the upper VB consists mainly of $2p_y$ orbitals of O atoms. Robertson and co-workers carried out first principle calculations using local density approximations (LDA) [32]. It is well known that LDA underestimate the bad gap energy, nevertheless these authors applied density functional methods which do give more accurate band gaps, as the GW approximation [33] or use an LDA with an exhange-correlation functional.

3.2. Surface models

From the optimized lattice structure, two symmetric and one asymmetric slabs of alternating SrO and ZrO_2 layers were built. The first symmetric slab was terminated by SrO planes and the second by ZrO_2 planes, Fig. 2a and 2b, respectively. There is mirror symmetry with respect to the central layer.

The asymmetric slab has the two possible terminations (no mirror symmetry is imposed), Fig. 2c. These slabs are finite in the z-direction but periodic in x and y-directions. The first problem to build the computational model is selecting the number of the layers in the slab. For this purpose, we have calculated the *cleavage energy*, E_s^u , following the definition of Heifets et al. [11] and also estimated the *relaxation energies*, $E_{rel}(i) = 1/2[\, E_{slab}(i) - E_{slab}^u(i)]$, for each possible symmetric termination, where $E_{slab}(i)$ is the slab energy after relaxation and the *surface energy*, $E_s(i) = E_s^u(i) + E_{rel}(i)$, calculated as the sum of the *cleavage* and *relaxation energies*, where i denotes SrO or ZrO_2. These energy calculations are used in Lazaro et al. [12].

Table 2 shows the results for the calculations of the *cleavage*, *relaxation* and *surface energies* for 5, 7, 9, 11, 13 and 15 layers. The results for the *cleavage energy* yields 1.97 eV/cell for $n = 9$ and 11, and 1.96 eV/cell for $n = 13$ and 15. The values found for the *surface energy*, at SrO terminated surfaces, are 1.17 eV/cell for $n = 9$, 11, 13 and 15 layers. On the other hand, for ZrO_2 terminated surface the calculated values are 1.75 and 1.74 eV/cell for n = 9 and 11, and 13 and 15 layers, respectively. The difference in *surface energy* is around 0.57 eV/cell, thus the ZrO_2 terminated is more stable than the SrO terminated surface. It is important to note that, a comparison of relative stability for both terminations is problematic since the corresponding surface model contains different number of atoms.

Consequently, 9 or 11-layers may be sufficient to describe the surface geometry and appropriate system for relaxation model studies. In addition, in order to confirm the convergence of the charge distribution with respect to slab thickness, we calculated the Mulliken charge distribution for the ZrO_2 and SrO terminated surface models. The analyses yields convergence for $n = 9$–15. Therefore, we have used an 11-layers slab model to describe the surface geometry and relaxation. For the asymmetric model we used 10 layers, whereas the first and last layers are ZrO_2 and SrO planes, respectively.

Table 3 summarizes the displacement in the z-direction (δz), obtained by relaxing all atoms of all layers. The positive displacement in the [001] directions denote relaxations towards the vacuum and the magnitudes are measured with respect to the bulk truncated atomic positions. The SrO terminated 11-layer surface indicates that the largest relaxations are on the first layer, which includes a displacement of Sr and O atoms of −0.46 and −0.05 Å, respectively. On the second layer the displacement of Zr and O atoms are 0.04 and −0.06 Å, respectively. The Sr atoms of the third layers have a significant displacement of −0.15 Å, whereas the O atoms have a displacement of −0.04 Å. The larger magnitude of Sr atom relaxation compared to O atoms leads to rumpling at the first and third surface layer.

For the ZrO_2 terminated 11-layer surface, the relaxations on the first layer shows a displacements of Zr and O atoms by −0.15 to −0.14 Å, respectively. At the subsurface layer, the relaxation of Sr and O atoms are 0.11 and −0.03 Å, respectively, leading to rumpling of second surface layers. At the third and fifth layers the Zr and O atoms

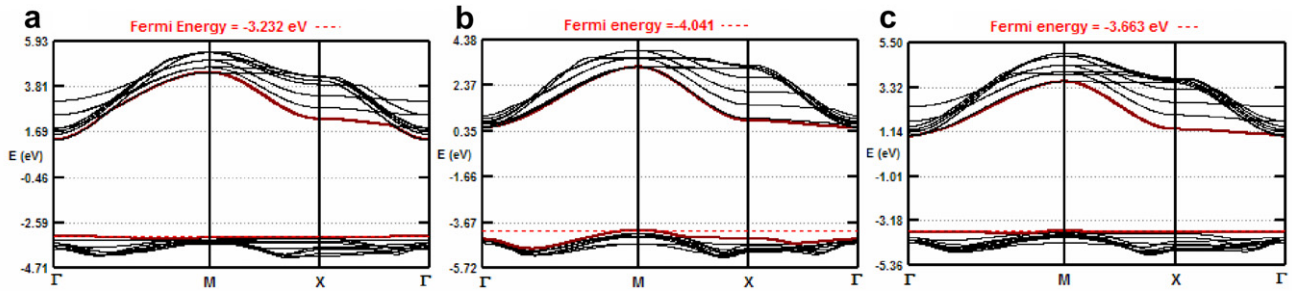

Fig. 3. Band structure of (a) SrO, (b) ZrO_2 and (c) asymmetric terminated surfaces.

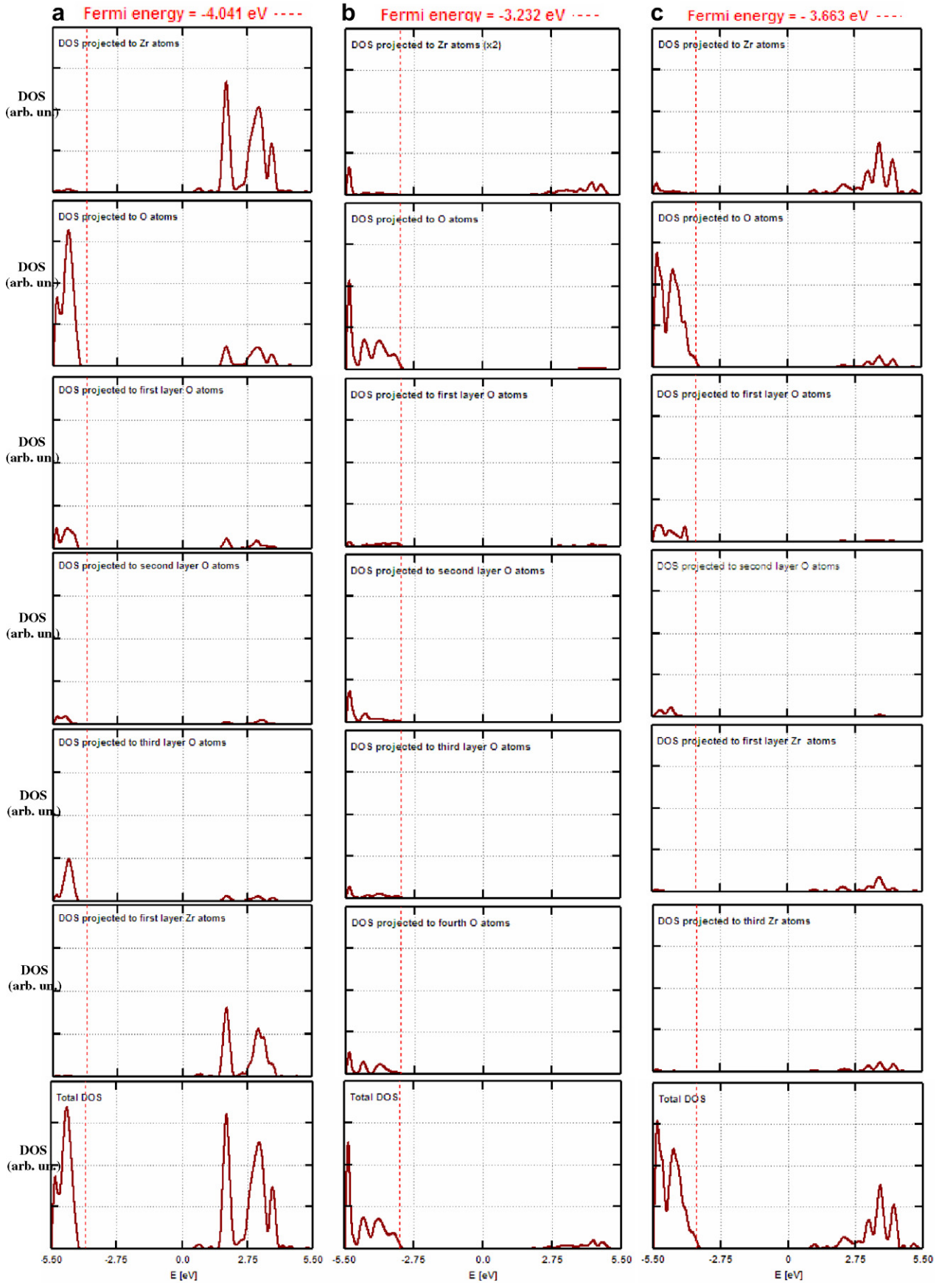

Fig. 4. Total and projected DOS of (a) SrO, (b) ZrO_2 and (c) asymmetric terminated surfaces.

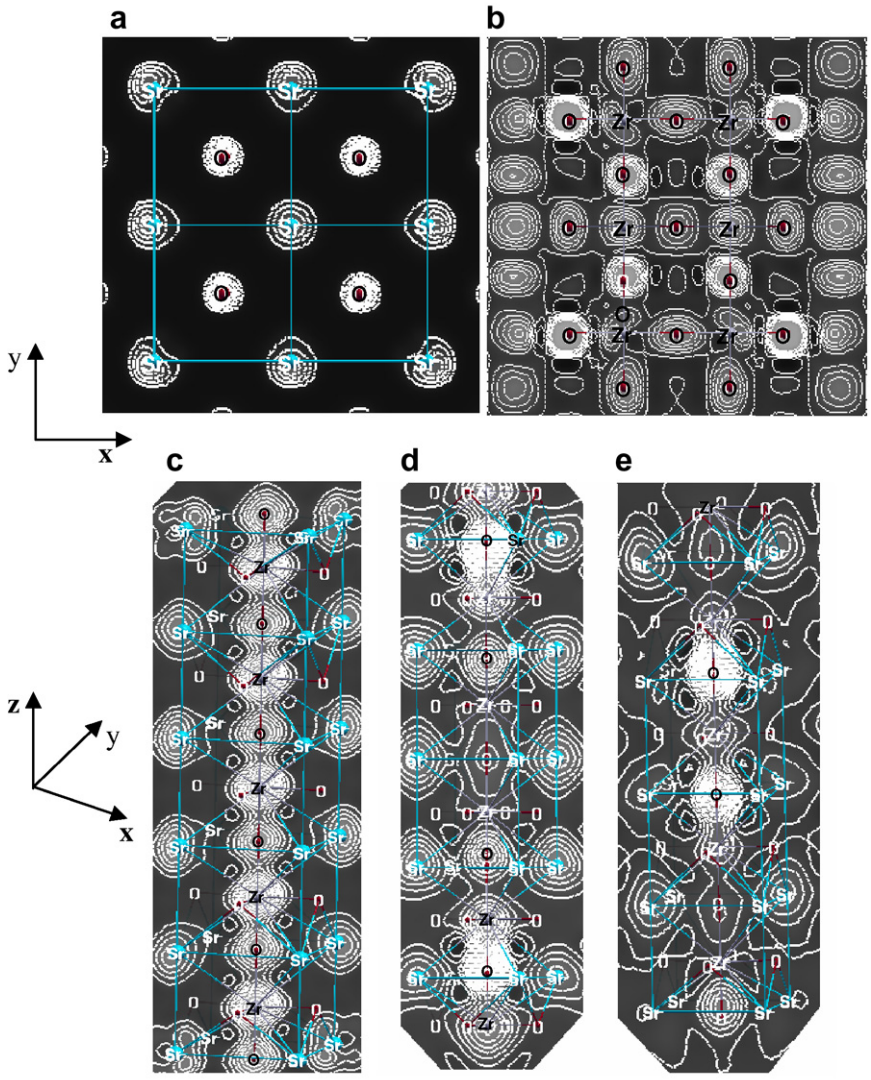

Fig. 5. Electron density maps of (a) SrO and (b) ZrO_2 terminated surfaces in the (001) plane and (c) SrO, (d) ZrO and (e) asymmetric terminated surfaces in the diagonal (110) plane.

Table 4
Distances (Å) of the Zr–O and Sr–O bonds of surface and subsurface layers, overlap populations (in $m|e|$) in parenthesis and Mulliken charge distribution, Q, (in $|e|$) for Bulk, ZrO_2, SrO and asymmetric terminations

	Bulk		ZrO_2 termination		SrO termination		Asymmetric termination	
1st layer	Sr–O 2.93 (7)		Zr–O 2.07 (84)		Sr–O 2.96 (9)		Zr–O 2.07 (84)	
Q	Sr 1.77	O −1.28	O −1.22	O −1.22	Sr 1.74	O −1.35	Zr 2.09	O −1.22
2nd layer	Zr–O 2.07 (76)		Sr–O 2.93 (6)		Zr–O 2.07 (66)		Sr–O 2.93 (6)	
Q	Zr 2.08	O −1.28	Sr 1.77	O −1.21	Zr 2.03	O −1.31	Sr 1.77	O −1.21
3rd layer	–		Zr–O 2.07 (79)		Sr–O 2.93 (7)		Zr–O 2.07 (79)	
Q	–		Zr 2.08	O −1.21	Sr 1.76	O −1.28	Zr 2.08	O −1.21
d_{12}	–		Zr–O 1.96 (116)		Zr–O 1.99 (118)		Zr–O 1.95 (116)	
d_{23}	–		Zr–O 2.06 (66)		Zr–O 2.04 (84)		Zr–O 2.11 (60)	

indicate displacements towards the bulk with the same direction and magnitude. The calculated displacement of the asymmetric 10-layer model yields the same displacement trends as the ZrO_2 terminated surface for the five first layers. The 10th, 9th, 8th, and 7th layers are equivalent to the 1st, 2nd, 3rd, and 4th layers of the SrO terminated sur-

face, respectively. At these layers the Sr and O atoms have similar displacement magnitudes but opposite directions (see Table 3).

We have also calculated and compared the relaxation for 9, 13 and 15-layers. If we compare 9 and 13-layer with the 11 and 15-layer slab models, it is observed that theses slab models are different with respect to the central layer. For the SrO terminated surfaces with 9 and 13 layers, the central layer consist of ZrO_2 planes. For the ZrO_2 terminated surfaces with 11 and 15-layers, the central layer consist of SrO planes. Composition and width, i.e., number of layers, affects the relaxation of external layers. A larger number of layers can yield greater freedom for the displacement of the external planes.

3.2.1. Band structure and density of states (DOS)

Fig. 3 shows the band structure for the three possible terminated relaxed surfaces, respectively. The top of the upper VB and the bottom of the lowest CB for SrO terminated surfaces (see Fig. 3a) is located at Γ point of the 2D Brillouin zone. The gap, compared with the bulk system becomes direct; yielding 4.536 eV. Thus, the band gap for SrO terminated surface is reduced. The top of the upper VB for the ZrO_2 (see Fig. 3b) terminated surface is located at the M point. The bottom of the lowest CB is located at the Γ point yielding an indirect gap of 4.562 eV. For the asymmetric slab model the gap is indirect yielding 4.637 eV, between M and Γ points. In a general the gap is reduced from 4.86 eV for the bulk to approximately 4.56 eV for the surfaces. The band structures are similar for all surfaces.

In order to understand the band structure, the DOS was calculated. Fig. 4 depicts the total and atom projected DOS for the three possible terminated surface structures. The analysis of the principal atomic orbital components (AO) of selected bands, are performed with a threshold of 15 a.u. for the important eigenvector coefficients. For SrO terminated surfaces, it is observed that the Sr atoms do not contribute. The AO contributions shows that the bands are mainly derived by $2p_y$ and $2p_z$ orbitals of O atoms. Compared with the total DOS (see Fig. 4a), the surface estates at the bottom of VB, clearly contribute to the 3d AO of surface Zr atoms. For ZrO termination, the projected DOS for the O atoms indicate that the main contribution of O 2p states are displaced to a lower energy range, compared with the bulk. The major contributions are derived from the second end fourth layer O atoms. The Sr and Zr atoms do not have significant contribution to the CB. For the asymmetric surface the main contribution to the VB and CB comes from the O 2p states of first and second layers and Zr 3d levels of first and third layers.

Fig. 5 shows the electron density in the surface plane for the SrO and ZrO_2 terminated surfaces. The contours show that there is no trace of covalent character between M = Sr or Zr and O surface atoms. On the other hand, the contour in the diagonal (110) plane indicates a covalent character between Zr and O atoms for the SrO terminated surface. The dipole moment is perpendicular to the surface due to the displacement of the Sr atoms in the surface layer. For the ZrO terminated surface, Fig. 5d, the contour in the diagonal plane indicates no trace of partial covalent character for the central layers and a covalent character for external layers. In the asymmetric model (see Fig. 5e) there is an inverse behavior. This fact is corroborated by the results presented in Table 4.

4. Summary

Computational studies, based on first principle calculations, can be important for elucidating the electronic and structural properties of materials. There is a more significant rumpling in the SrO as compared to the ZrO_2 terminated surfaces. Composition and width, i.e number of layers affects the relaxation of external layers. A larger number of layers can yield greater freedom for the displacement of the external planes. 9 or 11-layers may be sufficient to describe the surface geometry and appropriate systems for relaxation model studies. Relaxation of Sr and O atoms leads to rumpling of surface layers. The gap is indirect and reduced from 4.856 eV for the bulk to approximately 4.6 eV for the surfaces. DOS analyses indicate that the main contribution to the VB and CB comes from the O 2p states and Zr 3d levels. The ZrO_2 terminated surface appears to be more stable than the SrO terminated surface. The electron density maps show that there is no trace of covalent character between M = Sr or Zr and O surface atoms. The contour in the (110) diagonal plane indicates a partial covalent character between Zr and O atoms for the SrO terminated surface. For the ZrO_2 terminated surface, the contour in the diagonal plane indicates no trace of partial covalent character for the central layers and a covalent character for external layers.

References

[1] B.J. Kennedy, C.J. Howard, Phys. Rev. B 59 (1999) 4023.
[2] D. Souptel, G. Behr, A.M. Balbashov, J. Cryst. Growth 236 (2002) 583.
[3] E. Mete, R. Shaltaf, S. Ellialtioglu, Phys. Rev. B 68 (2003) 035119.
[4] J. Muscat, A. Wander, N.M. Harrison, Chem. Phys. Lett. 342 (2001) 397.
[5] J.R. Sambrano, J.B.L. Martins, J. Andres, E. Longo, Int. J. Quantum Chem. 85 (2001) 44.
[6] J.R. Sambrano, G.F. Nobrega, C.A. Taft, J. Andres, A. Beltran, Surf. Sci. 580 (2005) 71.
[7] J.R. Sambrano, E. Orhan, M.F.C. Gurgel, A.B. Campos, M.S. Goes, C.O. Paiva-Santos, J.A. Varela, E. Longo, Chem. Phys. Lett. 402 (2005) 491.
[8] R. Terki, H. Feraoun, G. Bertrand, H. Aourag, Phys. Status Solid B-Basic Solid State Phys. 242 (2005) 1054.
[9] R.A. Evarestov, A.V. Bandura, V.E. Aleksandrov, Phys. Solid State 47 (2005) 2248.
[10] R.A. Evarestov, A.V. Bandura, V.E. Alexandrov, E.A. Kotomin, Phys. Stat. Sol. (b) 242 (2005) R11.
[11] E. Heifets, R.I. Eglitis, E.A. Kotomin, J. Maier, G. Borstel, Phys. Rev. B 64 (2001) 235417.

[12] S. Lazaro, E. Longo, J.R. Sambrano, A. Beltran, Surf. Sci. 552 (2004) 149.
[13] S. Piskunov, E.A. Kotomin, E. Heifets, Microelectron. Eng. 81 (2005) 472.
[14] Y.X. Wang, M. Arai, T. Sasaki, C.L. Wang, Appl. Phys. Lett. 88 (2006) 091909.
[15] R.N. Schwartz, B.A. Wechsler, L. West, Appl. Phys. Lett. 67 (1995) 1352.
[16] T. Tybell, C.H. Ahn, J.M. Triscone, Appl. Phys. Lett. 72 (1998) 1454.
[17] A.D. Becke, J. Chem. Phys 98 (1993) 5648.
[18] C. Lee, W. Yang, R.G. Parr, Phys. Rev. B 37 (1988) 785.
[19] R. Dovesi, V.R. Saunders, C. Roetti, M. Causà, N.M. Harrison, R. Orlando, E. Aprà: CRYSTAL03 User's Manual, University of Torino, Torino, 2003.
[20] F. Corà, M. Alfredsson, G. Mallia, D.S. Middlemiss, W. Mackrodt, R. Dovesi, Orlando: Structure, Bonding, Springer, Verlag, Berlin, 2004.
[21] E. Orhan, V.C. Albarici, M.T. Escote, M.A.C. Machado, P.S. Pizani, E.R. Leite, J.R. Sambrano, J.A. Varela, E. Longo, Chem. Phys. Lett. 398 (2004) 330.
[22] Available from <http://www.tcm.phy.cam.ac.uk/~mdt26/crystal.html>.
[23] A.J. Smith, A.J.E. Welch, Acta Crystallographica 13 (1960) 653.
[24] J.A. Nelder, R. Mead, Comput. J. 7 (1965) 308.
[25] S. Piskunov, E. Heifets, R.I. Eglitis, G. Borstel, Comput. Mater. Sci. 29 (2004) 165.
[26] D. deLigny, P. Richet, Phys. Rev. B 53 (1996) 3013.
[27] N.L. Ross, R.J. Angel, J. Kung, T.D. Chaplin, Perovskite Materials, in: K. Poeppelmeier, A. Navrotsky, R. Wentzcovitch (Eds.), MRS Simposia. Material Research Society, 2002, p. D2.4.1.
[28] A.B. Alcagirov, J.P. Perdew, J.C. Boettger, R.C. Albers, C. Folhais, Phys. Rev. B 63 (2001) 224115.
[29] A. Kokalj, J. Mol. Graph. 17 (1999) 176.
[30] V.M. Longo, L.S. Cavalcante, A.T. de Figueiredo, L.P.S. Santos, E. Longo, J.A. Varela, J.R. Sambrano, C.A. Paskocimas, F.S. De Vicente, A.C. Hernandes, Appl. Phys. Lett. 90 (2007) 091906.
[31] Y.S. Lee, J.S. Lee, T.W. Noh, D.Y. Byun, K.S. Yoo, K. Yamaura, E. Takayama-Muromachi, Phys. Rev. B 67 (2003) 113101.
[32] J. Robertson, K. Xiong, S.J. Clark, Thin Solid Films 496 (2006) 1.
[33] M.S. Hybertsen, S.G. Louie, Phys. Rev. B 34 (1986) 5390.